

Theory of spin-wave excitation in manganites

Ryo Maezono and Naoto Nagaosa

Department of Applied Physics, University of Tokyo, Bunkyo-ku, Tokyo 113-8656, Japan

(Received 1 September 1999)

The role of the orbital degrees of freedom is studied theoretically for the spin dynamics of $R_{1-x}A_x\text{MnO}_3$. Based on the mean-field solution, a random-phase approximation calculation has been done and it is found that the $d_{x^2-y^2}$ -type orbital is essential for the double exchange (DE) interactions, i.e., the DE is basically a two-dimensional interaction. Based on this result compared with experiments, we propose that the orbital wave function is $d_{x^2-y^2}$ -type locally even in the metallic ferromagnetic state, which fluctuates quantum mechanically. Good agreement of the estimation with experiments suggests that the Jahn-Teller phonon has less importance on the spin dynamics.

Doped manganites $R_{1-x}A_x\text{MnO}_3$ ($R=\text{La, Pr, Nd, Sm}$; $A=\text{Ca, Sr, Ba}$) have recently attracted considerable interest due to the colossal magnetoresistance (CMR) observed near the ferromagnetic (spin F -type) transition temperature T_c .¹⁻⁴ It is now recognized that the most fundamental interaction in these materials is the double exchange interaction (DE), which connects the transport and magnetism.⁵ Therefore the magnetism is a key issue to reveal the mechanism of CMR. Especially, rich magnetic phase diagrams have been clarified over the wide range of the concentration x and also the bandwidth. With increasing x , the parent insulator with a layered antiferromagnetism (spin A -type AF) changes into a ferromagnetic metal (FM).⁶ In addition to these well-known magnetic phases, spin A -type AF [in $\text{La}_{1-x}\text{Sr}_x\text{MnO}_3$,⁷ $\text{Pr}_{1-x}\text{Sr}_x\text{MnO}_3$,^{8,9,20} $\text{Nd}_{1-x}\text{Sr}_x\text{MnO}_3$ (Ref. 10)] and the rod-type antiferromagnetism [spin C -type AF, in $\text{Nd}_{1-x}\text{Sr}_x\text{MnO}_3$ (Refs. 10,36)] were recently found in the moderately doped metallic region ($0.5 < x < 0.8$).

The neutron-scattering experiments have revealed the spin-wave excitation at low temperatures, which depends sensitively on the doping x and the magnetic structure.¹¹⁻¹⁸ In the spin A -type AF for small x , the dispersion is two dimensional while it becomes isotropic in the FM state. The spin stiffness, however, stays almost constant up to $x \cong 0.125$ where the phase transition between the insulating and metallic ferromagnetic states occurs.¹³ This phase transition is accompanied with that of the orbital structure.¹⁹ In the FM state, the orbital ordering disappears and the spin stiffness begins to increase. In the metallic A -type AF (AFM) state for higher x , the dispersion becomes again two dimensional.¹⁷ In this paper we report the calculation of the spin-wave dispersion by changing x and taking into account the orbital structure. The calculated x dependence of the spin stiffness agrees quantitatively with the observed one for $x \geq 0.2$ where the double exchange interaction dominates. This x dependence strongly supports the large orbital polarization, which is $d_{x^2-y^2}$ at least locally. Therefore the double exchange interaction is basically two dimensional.

We previously reported a mean-field theory (MFT) for the phase diagram of doped manganites in terms of a model including the strong on-site repulsion, orbital degeneracy, and anisotropic covalency.²⁰ Based on this MFT, we first present the spin-wave dispersion in terms of the random-

phase approximation (RPA). This reproduces qualitatively the x dependence of the stiffness and the anisotropy due to the crossover from superexchange interaction (SE) to DE. Especially for the doped region, only when the orbital configuration becomes $d_{x^2-y^2}$, i.e., $x \geq 0.2$, the DE becomes appreciable and the in-plane spin stiffness grows rapidly. Observed values of the in-plane spin stiffness^{11,16,17} agree quantitatively with the estimated value with $d_{x^2-y^2}$ -orbital ordering. This is understood in terms of the orbital liquid picture^{20,21} and implies that the Jahn-Teller (JT) phonon has less importance on the spin dynamics.

We start with the Hamiltonian

$$H = \sum_{\sigma\gamma\gamma'\langle ij \rangle} t_{ij}^{\gamma\gamma'} d_{i\sigma\gamma}^\dagger d_{j\sigma\gamma'} - J_H \sum_i \vec{S}_{t_{2g}i} \cdot \vec{S}_{e_gi} + J_S \sum_{\langle ij \rangle} \vec{S}_{t_{2g}i} \cdot \vec{S}_{t_{2g}j} + H_{\text{on-site}}, \quad (1)$$

where $\gamma = [a(d_{x^2-y^2}), b(d_{3z^2-r^2})]$ specifies the orbital and the other notations are standard. The transfer integral $t_{ij}^{\gamma\gamma'}$ depends on the pair of orbitals (γ, γ') and the direction of the bond (i, j).²¹ The spin operator for the e_g electron is defined as $\vec{S}_{e_gi} = \frac{1}{2} \sum_{\gamma\alpha\beta} d_{i\gamma\alpha}^\dagger \vec{\sigma}_{\alpha\beta} d_{i\gamma\beta}$ with the Pauli matrices $\vec{\sigma}$, while the orbital isospin operator is defined as $\vec{T}_i = \frac{1}{2} \sum_{\gamma\gamma'\sigma} d_{i\gamma\sigma}^\dagger \vec{\sigma}_{\gamma\gamma'} d_{i\gamma'\sigma}$. J_H is the Hund's coupling between e_g and t_{2g} spins, and J_S is the AF coupling between nearest-neighbor t_{2g} spins. $H_{\text{on-site}}$ represents the on-site Coulomb interactions between e_g electrons. Coulomb interactions induce both the spin and orbital isospin moments, and actually $H_{\text{on-site}}$ can be written as^{20,21}

$$H_{\text{on-site}} = - \sum_i (\tilde{\beta} \vec{T}_i^2 + \tilde{\alpha} \vec{S}_{e_gi}^2), \quad (2)$$

where the coefficients of the spin and isospin operators, i.e., $\tilde{\alpha}$ and $\tilde{\beta}$, are given by^{20,21} $\tilde{\alpha} = U - J/2 > 0$, and $\tilde{\beta} = U - 3J/2 > 0$. The parameters $\tilde{\alpha}, \tilde{\beta}, t_0$, used in the numerical calculation are chosen as $t_0 \sim 0.72$ eV, $U = 6.3$ eV, and $J = 1.0$ eV, being relevant to the actual manganites.²⁰

In the path-integral quantization, we introduce the Stratonovich-Hubbard fields $\vec{\varphi}_S$ and $\vec{\varphi}_T$, representing the spin and orbital fluctuations, respectively. With the large values of the electron-electron interactions above, both $\vec{\varphi}_S$ and $\vec{\varphi}_T$ are almost fully polarized.²⁰ The MFT corresponds to the saddle-point configuration of $\vec{\varphi}_S$ and $\vec{\varphi}_T$. We consider four kinds of spin alignment in the cubic cell: *F*, *A*, *C*, and *G* type. As for the orbital degrees of freedom, we consider two sublattices *I* and *II*, on each of which the orbital is specified by the angle $\theta_{I,II}$ as²⁰

$$|\theta_{I,II}\rangle = \cos \frac{\theta_{I,II}}{2} |d_{x^2-y^2}\rangle + \sin \frac{\theta_{I,II}}{2} |d_{3z^2-r^2}\rangle. \quad (3)$$

We consider four types, i.e., *F*, *A*, *C*, and *G* type also for the orbital ordering. Henceforth we use a notation such as spin *A*, orbital $G(\theta_I, \theta_{II})$ etc. In MFT, the most stable ordering is given by²⁰

| | | |
|-------------|---------------|------------------------------|
| $x=0.0$ | spin <i>A</i> | orbital <i>C</i> :(60, -60), |
| $x=0.1$ | spin <i>F</i> | orbital <i>C</i> :(80, -80), |
| $x=0.2-0.4$ | spin <i>A</i> | orbital <i>F</i> :(0,0), |
| $x=0.5-0.9$ | spin <i>C</i> | orbital <i>F</i> :(180,180). |

As for $x=0$, we further introduced the JT effect²⁰ by putting the observed distortion of the MnO_6 octahedra.²²

RPA corresponds to the Gaussian fluctuation around MFT, and the contribution to the spin-wave effective action from the e_g electrons S_{SW} is obtained as the expansion around the saddle point:

$$S_{\text{SW}} = \sum_{\vec{q}, \Omega} K_{\pi}(\vec{q}, \Omega) \vec{\pi}(\vec{q}_S + \vec{q}, \Omega) \cdot \vec{\pi}(-\vec{q}_S - \vec{q}, -\Omega) \\ + \sum_{\vec{q}, \Omega} K_{\times}(\vec{q}, \Omega) \vec{\pi}(\vec{q}_S + \vec{q}, \Omega) \cdot \{\vec{n} \times \vec{\pi}(-\vec{q}_S - \vec{q}, -\Omega)\}, \quad (4)$$

where $\vec{q}_S (\equiv -\vec{q}_S)$ is the wave vector and $\vec{n} (|\vec{n}|=1)$ is the direction of the ordered magnetic moment, and $\vec{\pi}$ is the fluctuation perpendicular to it. Because the spin wave is the Goldstone boson, the condition $K_{\pi}(0,0)=0$, $K_{\times}(0,0)=0$, can be derived. Coefficient of the diagonalized quadratic form is obtained as $K_{\uparrow(\downarrow)} = K_{\pi} \pm iK_{\times}$, zero point of which $[K_{\uparrow(\downarrow)}(\vec{q}, \Omega = -i\omega) = 0]$ gives the dispersion relation of the excitation $\omega = \omega(\vec{q})$. However, in this paper we focus on the *static* spin stiffness rather than the *dynamic* spin-wave velocity because (i) at $x=0$ the spin stiffness is correctly reproduced to be of the order of J in the RPA while the spin-wave velocity scales with t , and (ii) for the metallic region, $x \neq 0$, the Landau damping is not properly treated in our calculation where the Brillouin zone is discretized and thus the gapless individual excitation is not correctly evaluated. The *static* spin stiffness C_{α} corresponds to the static response function for small $|\vec{q}|$ as

$$\frac{K_{\sigma}(\vec{q}, \Omega=0)}{\tilde{\alpha}} \cong \sum_{\alpha=x,y,z} C_{\alpha} q_{\alpha}^2, \quad (5)$$

and roughly reflects the exchange interaction depending on x , where $\sigma=1(-1)$ corresponds to spin up (down), respectively.

In RPA calculation the SE corresponds to the contribution from the interband transitions, while the DE corresponds from the intraband ones. In this way, the present calculation describes both SE and DE interactions, and hence their crossover in a unified way. Also the contribution from J_S should be considered, the value of which is determined in the following way. We require that the experimentally observed anisotropy ratio of the spin stiffness $R = (D_{x,y}/D_z)^2$ is reproduced when the calculated contributions from e_g electrons and that from J_S are added. The observed value $R=7.6$ for LaMnO_3 (Ref. 15) leads to an estimation as $J_S = 0.997$ meV. As for AFM at $x=0.3$, the observed value $R=10.4$ for $\text{Nd}_{0.45}\text{Sr}_{0.55}\text{MnO}_3$ (Ref. 17) gives $J_S = 1.4$ meV. These estimations are consistent rather with $J_S \sim 0.8$ meV estimated from the Néel temperature of CaMnO_3 (Ref. 23) than the earlier mean-field estimations $J_S \sim 8$ meV.^{20,24} Using these estimations, $J_S \sim 1$ meV, we can estimate the spin-wave stiffness for $x=0$ as $J_{\text{total}}^x S_{\text{total}}^2 = 1.05$ meV, including the contribution from t_{2g} orbital. The corresponding experimental value is $J_{\text{total}}^x S_{\text{total}}^2 = 3.91$ meV in LaMnO_3 ,¹⁵ with the reported lattice constants and the magnitude of spin moment, $S_{\text{total}} = 3/2 + 1/2(1-x)$. The discrepancy may be attributed to the complex lattice deformations such as the Mn-O bond-length (JT-type distortion) and the Mn-O-Mn bond-angle (orthorhombic distortion) observed at $x=0$,¹⁵ which can also be an origin of the anisotropy.^{25,26}

We now turn to the doped case $x \neq 0$. Figure 1 shows the doping dependence of the total stiffness calculated for the optimized spin/orbital structure at each x . Firstly the spin stiffness due to the double exchange interaction scales roughly with x because the orbital is almost fully polarized, while in the absence of the orbital polarization it scales with the electron density $(1-x)$ rather than the hole x for small x . The observed stiffness enhancement with increasing x even in the metallic region¹³ therefore also supports the large orbital polarization due to the strong Coulomb interactions. As x increases, the spin structure changes from spin *A*-type insulator at $x=0$ into the nearly isotropic FM, to the AFM with two-dimensional $d_{x^2-y^2}$ orbital alignment, and to the spin *C* metal with $d_{3z^2-r^2}$ orbital.²⁰ Accordingly, the in-plane stiffness shows an increase, moderately at the beginning and then rapidly in the region of AFM. This reflects the fact that the DE is the most effective and prefers the $d_{x^2-y^2}$ orbital, i.e., the DE is basically *two dimensional* with the e_g orbitals. In the spin-*C* metal for $x > 0.4$, one-dimensional orbital along (001) direction gives rise to a steep increase of the stiffness in this direction.

The observed anisotropy of the spin stiffness is determined by the long-range ordering of the orbitals. Figure 1 also represents the crossover of the dimensionality which was proposed in the previous report.²⁰ Yoshizawa *et al.*¹⁷ observed the re-entrant of such two-dimensional anisotropy of the stiffness for $\text{Nd}_{0.45}\text{Sr}_{0.55}\text{MnO}_3$, being consistent with our result. Quasi-one-dimensional anisotropy is predicted for $\text{Nd}_{1-x}\text{Sr}_x\text{MnO}_3$ ($x > 0.6$).¹⁰

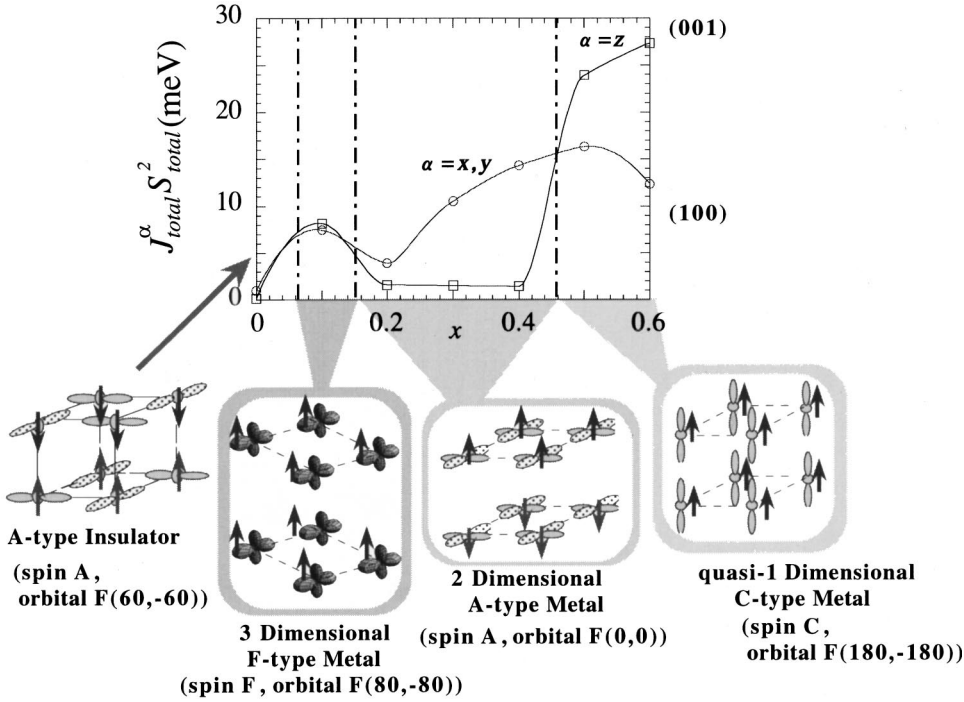


FIG. 1. Doping dependence of the spin stiffness. The orbital and the spin structure is optimized at each point. The enhancement of the spin stiffness and the cross-over of the dimensionality are seen with increasing x .

The in-plane spin stiffness $J_{\text{total}}^{\alpha} S_{\text{total}}^2$ in Fig. 1 could be compared with the experiments. In $\text{La}_{1-x}\text{Sr}_x\text{MnO}_3$, Endoh *et al.*¹³ observed the plateau of the velocity v_x in the orbital-ordered insulating state up to $x \sim 0.12$ and then the velocity increases in the FM phase. Comparing this with the calculation above, it seems that the moderate increase up to $x \sim 0.15$ in Fig. 1 corresponds to the plateau, while the rapid increase for $x > 0.15$ to the increasing velocity observed by Endoh.¹³ Then orbital-ordered FM state in Fig. 1 corresponds to the insulating spin F phase in experiments. Both the FM and AFM phases in experiments, on the other hand, seems to correspond to the AFM with $d_{x^2-y^2}$ orbital ordering in the calculation. This fits well orbital liquid picture by Ishihara *et al.*²¹; in a perfectly cubic system the orbital state in FM is described as the resonance among $d_{x^2-y^2}$, $d_{y^2-z^2}$, and $d_{z^2-x^2}$. In the actual CMR compounds, however, the slight lattice distortion^{11,16} may breaks the cubic symmetry to stabilize $d_{x^2-y^2}$ though it is still accompanied with large fluctuation around it.

Now we turn to the absolute value of the spin stiffness in FM phase. With the reported lattice constants the experimental values of the spin stiffness, $J_{\text{total}}^x S_{\text{total}}^2$, are 11.61 meV for $\text{La}_{0.7}\text{Sr}_{0.3}\text{MnO}_3$,¹¹ and 10.24 meV for $\text{Nd}_{0.7}\text{Sr}_{0.3}\text{MnO}_3$,¹⁶ respectively. These are in a good agreement with $J_{\text{total}}^x S_{\text{total}}^2 = 10.53$ meV estimated by RPA here with $x = 0.3$, $d_{x^2-y^2}$ -orbital ordering (a simple tight-binding estimation with $d_{x^2-y^2}$ -orbital also gives similar value). This agreement implies the large orbital polarization in FM phase with $d_{x^2-y^2}$ at least locally.

This orbital liquid picture also explains the spin-wave softening^{16,18,29} and spin canting³⁰ observed in this system. Some theoretical works shows that the orbital fluctuation in such an orbital liquid state leads to the softening of the spin-wave dispersion near the zone boundary²⁷ with the anisotropic feature²⁸ [the softening almost disappears along (π, π, π) directions^{18,29}]. As for the spin canting, the observed canting in the metallic region ($\text{Nd}_{0.5}\text{Sr}_{0.5}\text{MnO}_3$) with

the FM/AFM transition³⁰ cannot be explained unless the planer orbital $d_{x^2-y^2}$ realizes in FM phase³¹ (observed slight lattice anisotropy cannot stabilize such a planer orbital without the occurrence of the orbital liquid state).

An important conclusion from the agreement between the experiments and RPA calculation of the stiffness constant is that the polaron effect is small in the metallic state³² at least on the spin dynamics. Polaron should reduce the DE interaction in the doped region via a bandwidth reduction by a factor of $\langle X_i^\dagger X_j \rangle = \exp[-\sum_q |u_q|^2/2]$ [$u_q = (g_q/\omega_q)(e^{iq \cdot R_i} - e^{iq \cdot R_j})$], where $X_i = \exp[\sum_q e^{iq \cdot R_i} (g_q/\omega_q)(b_q - b_{-q}^\dagger)]$ is a factor encountered in the canonical transformation eliminating the coupling between electrons and polaronic bosons, $\sum_{i,\sigma} \sum_q g_q (b_q + b_{-q}^\dagger) d_{i\sigma}^\dagger d_{i\sigma}$, with the coupling constant g_q and phonon frequency ω_q .³³ On the other hand, for $x = 0$, the SE under the coupling with the polaron is given by

$$J = 4 |t_{ij}|^2 \int_0^\beta d\tau G_0^2(\tau) \langle X_i^\dagger(\tau) X_j(\tau) X_j^\dagger(0) X_i(0) \rangle, \quad (6)$$

where $G_0(\tau) = e^{-U\tau/2}$ is the Green's function for localized electrons. Because we are interested in the large U case, the integral is determined by the small τ region where $\langle X_i^\dagger(\tau) X_j(\tau) X_j^\dagger(0) X_i(0) \rangle \cong e^{-\tilde{\Delta}\tau}$ ($\tilde{\Delta} = \sum_q \omega_q |u_q|^2$). Then the polaronic effect is to replace U by $U + \tilde{\Delta}$ in the expression for J , which is a minor correction when $U \gg \tilde{\Delta}$,³⁴ being in sharp contrast to DE discussed above. Polaronic effect should therefore correct the RPA estimation of the stiffness enhancement as x increases to be smaller. Agreement between the observed and estimated stiffness for DE implies therefore that the spin dynamics is not so affected by the polaron. This is also pointed out by Quijada *et al.*³⁵

In summary, we have studied the role of orbitals in the spin dynamics of $R_{1-x}A_x\text{MnO}_3$. Comparing the experiments with the RPA calculation based on the mean field theory, we conclude the following. (i) x dependence of the stiffness en-

hancement suggests the large orbital polarization. (ii) The double exchange interaction prefers $d_{x^2-y^2}$ orbital and is basically a two-dimensional interaction, which leads to the large anisotropy of the spin dynamics. (iii) The agreement between experiments and RPA results strongly suggests that the spin dynamics is not so affected by the JT polaron.

The authors would like to thank K. Hirota, Y. Endoh, I. Solov'ev, K. Terakura, R. Kajimoto, H. Yoshizawa, T. Kimira, D. Khomskii, A. Millis, and Y. Tokura for their valuable discussions. This work was supported by Priority Areas Grants from the Ministry of Education, Science and Culture of Japan.

-
- ¹K. Chahara, T. Ohono, M. Kasai, Y. Kanke, and Y. Kozono, *Appl. Phys. Lett.* **62**, 780 (1993).
- ²R. von Helmolt, J. Wecker, B. Holzapfel, L. Schultz, and K. Samwer, *Phys. Rev. Lett.* **71**, 2331 (1993).
- ³A. Urushibara, Y. Moritomo, T. Arima, A. Asamitsu, G. Kido, and Y. Tokura, *Phys. Rev. B* **51**, 14 103 (1995).
- ⁴S. Jin, T. H. Tiefel, M. McCormack, R. A. Fastnacht, R. Ramesh, and L. H. Chen, *Science* **264**, 413 (1994).
- ⁵P.G. de Gennes, *Phys. Rev.* **118**, 141 (1960).
- ⁶G.H. Jonker and H. van Santen, *Physica (Amsterdam)* **16**, 337 (1950).
- ⁷Y. Moritomo, T. Akimoto, A. Nakamura, K. Ohoyama, and M. Ohashi, *Phys. Rev. B* **58**, 5544 (1998).
- ⁸H. Kawano, R. Kajimoto, H. Yoshizawa, T. Tomioka, H. Kuwahara, and Y. Tokura, *Phys. Rev. Lett.* **78**, 4253 (1997).
- ⁹Y. Tomioka *et al.* (unpublished).
- ¹⁰H. Kuwahara, T. Okuda, Y. Tomioka, T. Kimura, A. Asamitsu, and Y. Tokura, in *Science and Technology of Magnetic Oxides*, edited by M. Hundley, J. Nickel, R. Ramesh, and Y. Tokura, MRS Symposia Proceedings No. 494 (Materials Research Society, Pittsburgh, 1998), p. 83.
- ¹¹M.C. Martin, G. Shirane, Y. Endoh, K. Hirota, Y. Moritomo, and Y. Tokura, *Phys. Rev. B* **53**, R14 285 (1996).
- ¹²T.G. Perring, G. Aeppli, S. M. Hayden, S. A. Carter, J. P. Remeika, and S.-W. Cheong, *Phys. Rev. Lett.* **77**, 711 (1996).
- ¹³Y. Endoh and K. Hirota, *J. Phys. Soc. Jpn.* **66**, 2264 (1997).
- ¹⁴K. Hirota, N. Kaneko, A. Nishizawa, Y. Endoh, M. C. Martin, and G. Shirane, *Physica B* **237-238**, 36 (1997).
- ¹⁵K. Hirota, N. Kaneko, A. Nishizawa, and Y. Endoh, *J. Phys. Soc. Jpn.* **65**, 3736 (1996).
- ¹⁶J.A. Fernandez-Baca, P. Dai, H. Y. Hwang, C. Kloc, and S.-W. Cheong, *Phys. Rev. Lett.* **80**, 4012 (1998).
- ¹⁷H. Yoshizawa, H. Kawano, J. A. Fernandez-Baca, H. Kuwahara, and Y. Tokura, *Phys. Rev. B* **58**, R571 (1998).
- ¹⁸H.Y. Hwang, P. Dai, S.-W. Cheong, G. Aeppli, D. A. Tennant, and H. A. Mook, *Phys. Rev. Lett.* **80**, 1316 (1998).
- ¹⁹Y. Endoh, K. Hirota, S. Ishihara, S. Okamoto, Y. Murakami, A. Nishizawa, T. Fukuda, H. Kimura, H. Nojiri, K. Kaneko, and S. Maekawa, *Phys. Rev. Lett.* **82**, 4328 (1999).
- ²⁰R. Maezono, S. Ishihara, and N. Nagaosa, *Phys. Rev. B* **57**, R13 993 (1998); **58**, 11 583 (1998).
- ²¹S. Ishihara, M. Yamanaka, and N. Nagaosa, *Phys. Rev. B* **56**, 686 (1997).
- ²²G. Matsumoto, *J. Phys. Soc. Jpn.* **29**, 606 (1970).
- ²³J.B. Goodenough, *Phys. Rev.* **100**, 564 (1955).
- ²⁴S. Ishihara, J. Inoue, and S. Maekawa, *Phys. Rev. B* **55**, 8280 (1997).
- ²⁵I. Solov'ev, N. Hamada, and K. Terakura, *Phys. Rev. Lett.* **76**, 4825 (1996).
- ²⁶H. Sawada, Y. Morikawa, K. Terakura, and N. Hamada, *Phys. Rev. B* **56**, 12 154 (1997).
- ²⁷G. Khaliullin and R. Kilian, cond-mat/9904316, *Phys. Rev. B* (to be published).
- ²⁸N. Nagaosa (unpublished).
- ²⁹P. Dai, H. Y. Hwang, J. Zhang, J. A. Fernandez-Baca, S. -W. Cheong, C. Kloc, Y. Tomioka and Y. Tokura, cond-mat/9904372 (unpublished).
- ³⁰H. Kawano *et al.*, cond-mat/9808286 (unpublished).
- ³¹R. Maezono and N. Nagaosa, cond-mat/9904427, *Phys. Rev. B* (to be published 15 Jan 2000).
- ³²A.J. Millis, P. B. Littlewood, and B. I. Shraiman, *Phys. Rev. Lett.* **74**, 5144 (1995).
- ³³G. D. Mahan, in *Many-Particle Physics*, 2nd. ed. (Plenum Press, New York, 1990), Chap. 4.
- ³⁴K.I. Kugel, and D. I. Khomskii, *Zh. Éksp. Teor. Fiz.* **79**, 987 (1980) [*Sov. Phys. JETP* **52**, 501 (1981)].
- ³⁵M. Quijada, J. Yv Cerne, J. R. Simpson, H. D. Drew, K.H. Ahn, A. J. Millis, R. Shreekala, R. Ramesh, M. Rajeswari, and T. Venkatesan, *Phys. Rev. B* **58**, 16 093 (1998).
- ³⁶R. Kajimoto, H. Yoshizawa, H. Kawano, H. Kuwahara, Y. Tokura, K. Ohoyama, and M. Ohashi, *Phys. Rev. B* **60**, 9506 (1999).